PNAS
www.pnas.org

Supplementary Information for

Acyl-CoA Synthetase 6 enriches the neuroprotective omega-3 fatty acid DHA in the brain.

Regina F Fernandez, Sora Q Kim, Yingwei Zhao, Rachel M Foguth, Jessica L Counihan, Marcus M Weera, Daniel K Nomura, Julia A Chester, Jason R Cannon, Jessica M. Ellis

Jessica M. Ellis
Email: ellisje18@ecu.edu

This PDF file includes:

Supplementary text
Figs. S1 to S2
Tables S1 to S2
References for SI reference citations

www.pnas.org/cgi/doi/10.1073/pnas.1807958115

Supplementary Information

Supplemental Methods.

ACS Assay: Total membrane fraction was prepared from midbrain and cortex. Acyl-CoA synthetase activity was measured in membrane fractions (5ug) incubated at 37°C for 5 minutes with 5mM ATP, 0.5mM CoA, 1mM DTT, 10mM $Mgcl_2$, 50mM Tris, and 0.05mM fatty acid: [1-^{14}C]Oleate (PerkinElmer), [1-^{14}C]Palmitate (PerkinElmer), [1-^{14}C] Arachidonic Acid (American Radiolabeled Chemicals), or [1-^{14}C] Docosahexaenoic Acid (Moravek) performed as described (1).

Behavioral Assessment: *Wire Hang Test:* Mice on a cage top were flipped, leaving the mice upside-down, and the latency to fall was recorded and multiplied by body weight to determine the minimal holding impulse (2). One training and four testing sessions were performed, each with three trials. *Adhesive Removal Test:* Performed as described, (3). *Open Field:* Mice were monitored in open field apparatus over 20 minutes using the MotorMonitor instrument (Kinder Scientific). *Whole-limb Grip Strength:* The gripping strength, defined as the peak force (N), was recorded for 4-5 trials, and the average was calculated (4). *Pre-Pulse Inhibition:* Pre-pulse inhibition was assessed using the Kinder Startle Monitor equipment (Coulbourn Instruments) using the protocol as described (5). *Fear Potentiated Startle*: Using the Coulbourn Instruments Animal Acoustic Startle System (Allentown, PA) as described (6). Briefly, mice were exposed to light or acoustic stimuli paired with (conditioning) or without (fear) electrical stimuli to the foot pad and the startle response was recorded.

Immunoblots and Histology: Sub-cellular fractionations were collected from mouse brain homogenates through a series of centrifugation and lysis steps according to (7). Mouse tissue lysates or membrane fractions were collected in lysis buffer (50mM Tris-HCl, 150mM NaCl, 1mM EDTA, and 1% Triton X-100) and sucrose medium (10mM Tris, 1mM EDTA, and 250mM sucrose), respectively. Protein concentration was quantified using Pierce BCA Protein Assay Kit (Thermo Fisher Scientific). 18ug of protein were subjected to SDS PAGE electrophoresis, transferred to nitrocellulose membranes, and blocked for 1 hour with 3% Bovine Serum Albumin-TBST (Tris Buffered saline, 0.1% Tween 20). The membrane were probed for primary antibody (1:1000) ACSL6 (raised against the peptide CNLLKQSEEVEDGGGAR), heat shock protein 60 (Santa Cruz), and beta-tubulin (Sigma), washed with 5% milk-TBST, and incubated with anti-mouse or anti-rabbit IRDye-conjugated secondary antibodies (LiCor). Membranes were exposed to Odyssey (LiCor) instrument and protein was quantified using LiCor software. For immunohistochemistry, brains were surgically removed, post-fixed in 4% PFA for 7 days, and then saturated with 30% sucrose at 4 °C for at least 7 days. Each brain was coronally sectioned on a frozen sliding microtome (Microm HM 450, Thermo Scientific) at a 35 μm thickness and stored in cryoprotectant at −20 °C. Brain sections containing cerebellum were randomly selected, rinsed 6 times with PBS at RT for 10 min at RT with shaking; blocked in 10% normal donkey serum (NDS) in PBS-T (0.3%) for 1hr at RT; incubated with primary antibodies (GFAP, abcam 134014; NeuN abcam 53554; tyrosine hydroxylase, Millipore AB1542; Iba1, Wako WEE4506) for 24-48 h in PBS-T with 1% NDS at 4 °C; rinsed 3 times with PBS at RT for 10 min; incubated with secondary antibodies (Alexa Fluor 488 anti-goat; Alexa Fluor 647 anti-chicken; Cy3 anti-sheep; Alexa Fluor 488 anti-rabbit from ImmunoJackson Laboratories, and sheep anti-Dylight800 from Rockland 613-745-168) in PBS-T with 1% NDS for 2hrs at RT; and rinsed 6 times with PBS at RT for 10 min each time before mounting on slides. Slides were dehydrated in graded alcohol and histoclear before coverslipped. Images were captured on an inverted Nikon D-Eclipse C1 confocal microscope. All slides were scanned under the same conditions for magnification, exposure time, lamp intensity and camera gain. For GFAP fluorescence quantification, a core of white matter (the arbor vitae) was analyzed. Mean intensity of fluorescence of GFAP+ cells and area fraction occupied by GFAP+ within arbor vitae were obtained by using NIS-Elements Basic Research software (Nikon). Mean intensity value is a statistical mean of intensity values of pixels derived from the intensity histogram. GFAP immunoreactivity was quantified by determining mean intensity of fluorescence of GFAP+ cells and area fraction occupied by GFAP+ in white matter of cerebellum with the NIS-Elements Basic Research software (Nikon). Briefly, white matter of cerebellum was delineated as region of interest and the binary overlay of GFAP+ cells was created by defining the threshold for background correction. For all images, same threshold value was established at the level at which the binary overlay entirely encloses the cell body and projections. Thus, mean intensity of the binary images were used for GFAP immunoreactivity and the area fraction of GFAP immunoreactivity was calculated by dividing the binarized GFAP+ area by the area occupied by the outlined region of interest and expressed as a percentage. For electron microscopy, the cerebellum was processed, stained, and prepared for transmission electron microscope with the Life Sciences Microscope Facility at Purdue. Images were captured on a FEI Tecnai G2 20 Transmission Electron Microscope.

RT-PCR: Total tissue RNA was extracted using TRIzol (Life Technologies), purified (PureLink RNA Mini Kit, Life Technologies), quantified by NanoDrop 2000 spectrophotometer (ThermoFisher Scientific), and use to synthesize cDNA with High Capacity cDNA Reverse Trancriptase (Applied Biosystems). Real-Time PCR was performed using SYBR Green Master Mix (Bio-Rad) and primers for the target genes and analyzed by using a StepOnePlus Real Time PCR System thermocycler (Applied Biosystems). Gene expression was normalized to the average Ct values of the housekeeping gene Rpl22 and expressed as $2^{-\Delta}$CT.

Lipidomics: Data presented in Figure 3 and supplemental Table 1, performed as previously described (8). Nonpolar lipid metabolites from mouse cerebellum were extracted in chloroform/methanol/PBS (2:1:1, v/v/v, 4ml) with the addition of 10nmol internal standards dodecylglycerol and pentadecanoic acid (Santa Cruz Biotechnology and Sigma-Aldrich, respectively). The organic layer was separated from the aqueous layer by centrifugation at 1000g for 5 min, dried down under flowing nitrogen, and resuspended in 120μl of chloroform. 10ul aliquots were analyzed by liquid chromatography as previously described (8-10). Metabolites separation from mouse hippocampus was obtained using a Luna reverse-phase C5 column (50 × 4.6 mm and 5 μm diameter particles, Phenomenex). Mobile phase A was composed of water/methanol (95:5, v/v) and mobile phase B of isopropanol:methanol:water (60:35:5, v/v/v). Solvent modifiers 0.1% formic acid with 5 mM ammonium formate and 0.1% ammonium hydroxide were used to facilitate ion formation in addition to improving the LC resolution in both positive and negative ionization modes, respectively. Mass spectrometry (MS) analysis was performed on an Agilent 6430 QQQ LC-MS/MS (Agilent Technologies). Metabolites were identified by SRM of the transition from precursor to product ions at associated optimized collision energies and retention times as previously described (9, 10). Metabolites quantification was performed by integrating the area under the curve followed by normalization to internal standard values. Results are expressed as relative levels compared to controls. Lipid profiling presented in Figure 4 was performed with Purdue's Bindley Metabolite Profiling Facility. Lipids were extracted from tissues using Bligh and Dyer Method (11), The lipid phase was dried, resuspended and injected through a micro-autosampler (G1377A) into a QQQ6410 triple quadrupole mass spectrometer (Agilent Technologies, San Jose, CA) operated in the positive ion mode and equipped with Jet stream ESI ion source (12). Data was analyzed by calculating the percent distribution for each ion (ion peak of m/z intensity/total ion intensity).

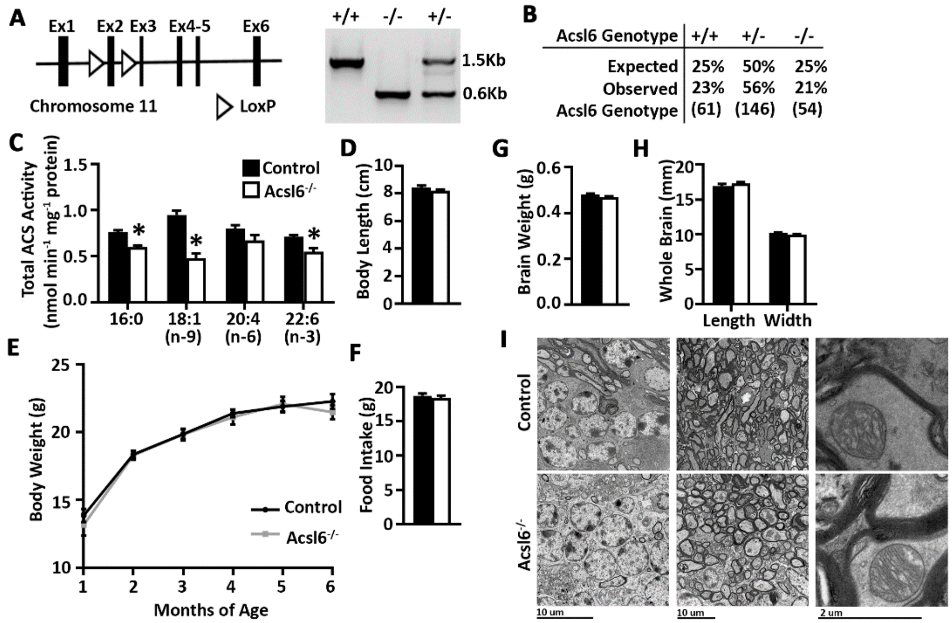

Fig. S1. (A) Schematic of Acsl6 targeting construct and representative PCR genotyping results of control, Acsl6-/-, and heterozygous mice. **(B)** Mendelian ratios for Acsl6 heterozygous mating. **(C)** Initial rate of ACS activity for [14C]16:0, [14C]18:1n9, [14C]20:4n-6, and [14C]22:6n-3 from control and Acsl6-/- cortex, n=5-6. **(D)** Body length from 2-month old control and Acsl6-/-, n=13-14, **(E)** Body weight over time of female control and Acsl6-/-, n=13-14. **(F)** Daily food intake of 5-6-month old control and Acsl6-/-, n=13-14. **(G)** Brain weight, **(H)** length, and width from 2-month old control and Acsl6-/-, n=13-14. **(I)** TEM images representing granular neurons (left), myelinated axons (middle), and axonal mitochondria (right). Data represent averages ± SEM; *, $p \leq 0.05$ by Student's t-test.

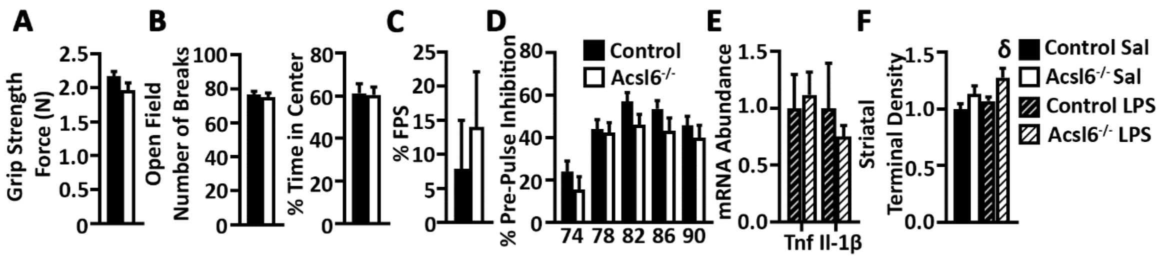

Fig. S2. (A) Forelimb grip strength in Newtons (N) for 4-5-month old control and Acsl6-/- mice, n=10. **(B)** Number of breaks (left) and percent time spent in the center (right) in the open field over a 20-minute period for 6-month old control and Acsl6-/- mice. **(C)** Fear potentiated startle and **(D)** percent pre-pulse inhibition in in 6-month old control and Acsl6-/- mice, n=28-30. **(E)** mRNA abundance of inflammatory genes in control and Acsl6-/- LPS treated 2-month old male mice, n=3. **(F)** Striatal terminal density of control and Acsl6-/- 6-month old mice injected with saline or LPS, n=5. Data represent averages ± SEM* by genotype, δ by treatment, p≤0.05 by Student's t-test.

Table S1. ACS Assay optimization: Total counts of radiation from ACS assay optimization on brain using oleate as substrate at a concentration of 50uM.

		Triton-X		
		0.5	**1**	**5**
ATP	**1**	2012		
	5	1939	1937	2153
	20		-183	
	50			-140
Time	**5**	2244		
	10	3070		
Protein	**10**	18189		
	20	34938		
	40	58715		
	60	79180		

Table S2. Lipidomic profile of 2-month old female cerebellum with or without overnight fasting, expressed as fold change in the Acsl6-/- brains relative to the control samples, n=5-6. Data represent averages ± SEM; significance represents Student's t-test between genotypes.

Supplemental Table 2.

Lipid Species	Control Fed	Acsl6-/- Fed	Control Fast	Acsl6-/- Fast
C16:0 FFA	1±0.06	0.96±0.05	0.96±0.07	0.93±0.05
C18:1 FFA	1±0.04	1.22±0.12	1.07±0.03	1.19±0.11
C18:0 FFA	1±0.05	1.00±0.03	1.10±0.09	1.04±0.05
C20:4 FFA	1±0.03	1.15±0.06[a]	1.12±0.08	1.10±0.08
C20:0 FFA	1±0.46	1.06±0.26	1.15±0.25	0.89±0.14
C22:6 FFA	1±0.16	0.56±0.08[a]	1.00±0.16	0.58±0.10[a]
C22:0 FFA	1±0.14	1.06±0.13	1.02±0.10	1.01±0.15
C24:0 FFA	1±0.10	0.93±0.14	0.91±0.18	0.78±0.10
C20:5 FFA	1±0.10	0.94±0.10	0.95±0.07	1.03±0.25
C22:6 FFA	1±0.14	0.45±0.03[a]	1.13±0.08	0.59±0.13[a]
C16:0 LPA	1±0.25	0.79±0.18	1.28±0.21	0.97±0.17
C18:1e LPAe	1±0.13	0.96±0.17	1.26±0.16	1.18±0.17
C18:0e LPAe	1±0.22	0.99±0.23	0.98±0.27	0.51±0.15
C18:1 LPA	1±0.18	0.76±0.18	1.21±0.23	1.02±0.23
C18:0 LPA	1±0.22	0.70±0.14	1.15±0.15	0.84±0.12
C20:4 LPA	1±0.07	1.18±0.25	1.38±0.16	1.13±0.09
C22:6 LPA	1±0.09	1.05±0.11	1.22±0.09	1.00±0.14
C16:0 LPI	1±0.26	0.79±0.21	1.34±0.29	1.07±0.28
C18:1 LPI	1±0.17	1.08±0.22	1.34±0.20	1.30±0.33
C18:0 LPI	1±0.16	0.83±0.18	1.46±0.23	1.13±0.22
C20:4 LPI	1±0.20	0.77±0.18	1.45±0.25	1.04±0.25
C18:2 LPI	1±0.15	1.31±0.31	1.38±0.20	1.18±0.31
C20:5 LPI	1±0.16	1.39±0.40	2.03±0.51	0.86±0.22
C22:6 LPI	1±0.12	0.28±0.08[a]	1.33±0.23	0.21±0.04[a]
C20:4 LPC	1±0.12	1.02±0.13	0.83±0.07	1.02±0.06
C18:1e LPCe (lysoPAF)	1±0.14	0.99±0.12	1.12±0.10	1.21±0.07
C20:0 LPC	1±0.15	0.82±0.12	1.01±0.10	1.03±0.09
C16:0e LPCe	1±0.10	0.90±0.06	1.06±0.06	1.06±0.04
C16:0e LPCe (lysoPAF)	1±0.11	0.92±0.06	0.94±0.06	1.07±0.03[b]
C16:0 LPC	1±0.16	0.77±0.12	0.95±0.11	0.99±0.09
C18:1e LPCe	1±0.18	0.83±0.10	1.04±0.14	0.94±0.09

C18:0e LPCe (lysoPAF)	1±0.09	0.99±0.14	1.18±0.10	1.36±0.12
C18:0e LPCe	1±0.16	0.67±0.11	0.94±0.10	0.97±0.09
C18:1 LPC	1±0.14	0.86±0.11	0.89±0.07	1.00±0.07
C18:0 LPC	1±0.16	0.77±0.12	1.00±0.10	1.00±0.09
C18:2 LPC	1±0.16	1.53±0.65	1.60±0.38	1.24±0.32
C20:5 LPC	1±0.08	0.87±0.08	0.79±0.07	0.80±0.06
C22:6 LPC	1±0.05	0.36±0.03[a]	1.15±0.21	0.50±0.10[a]
C18:2 LPG	1±0.03	1.33±0.11[a]	1.34±0.13[b]	1.54±0.14
C20:5 LPG	1±0.06	0.94±0.11	1.15±0.25	0.99±0.10
C22:6 LPG	1±0.05	0.36±0.03[a]	1.14±0.21	0.50±0.10[a]
C18:0e LPSe	1±0.10	1.01±0.20	1.08±0.20	1.15±0.11
C16:0 LPS	1±0.20	0.83±0.18	1.98±0.15	0.96±0.14
C18:1 LPS	1±0.19	0.75±0.17	1.06±0.19	0.94±0.19
C18:0 LPS	1±0.27	0.70±0.22	1.06±0.20	0.95±0.29
C18:2 LPS	1±0.05	0.49±0.05[a]	1.08±0.15	0.63±0.07[a]
C20:4 LPS	1±0.08	1.03±0.16	1.11±0.14	1.28±0.14
C20:5 LPS	1±0.10	1.17±0.10	1.01±0.26	1.22±0.11
C22:6 LPS	1±0.14	0.75±0.27	1.31±0.36	0.55±0.14
C22:6 LPS	1±0.15	0.75±0.27	1.31±0.37	0.56±0.15
C16:0e LPEe	1±0.15	0.83±0.15	1.04±0.12	1.11±0.12
C16:0 LPE	1±0.20	0.78±0.15	1.70±0.11	1.03±0.13
C18:1e LPEe	1±0.15	0.91±0.17	1.13±0.12	1.19±0.13
C18:0e LPEe	1±0.16	0.92±0.19	1.19±0.14	1.33±0.16
C18:0 LPE	1±0.17	0.87±0.17	1.15±0.11	1.28±0.19
C18:2 LPE	1±0.09	0.85±0.09	0.94±0.08	0.93±0.07
C20:4 LPE	1±0.15	1.47±0.31	1.13±0.15	1.77±0.36
C22:6 LPE	1±0.05	0.98±0.13	0.99±0.11	0.98±0.08
C18:1 LPE	1±0.13	1.05±0.15	1.03±0.11	1.24±0.14
C16:0e/18:1 PAe	1±0.08	1.12±0.20	1.21±0.11	1.13±0.10
C16:0/C18:1 PA	1±0.09	1.02±0.15	1.17±0.12	1.06±0.09
C16:0e/20:4 PAe	1±0.13	0.95±0.16	1.10±0.09	0.85±0.07[a]
C18:0e/C18:1 PAe	1±0.09	1.09±0.19	1.19±0.11	1.13±0.12
C16:0/C20:4 PA	1±0.05	0.87±0.13	1.03±0.10	0.91±0.07
C18:0/C18:1 PA	1±0.11	1.04±0.16	1.14±0.11	1.08±0.10
C18:0e/C20:4 PAe	1±0.10	0.98±0.16	1.07±0.09	0.97±0.11
C18:0/C20:4 PA	1±0.10	0.91±0.13	1.08±0.11	0.99±0.09
C16:0/C18:2 PA	1±0.07	1.35±0.14	1.18±0.05	1.25±0.13
C18:0/C18:2 PA	1±0.05	1.10±0.09	1.14±0.07	1.08±0.08

C16:0/C16:0 PI	1±0.14	1.03±0.16	1.04±0.11	1.01±0.14
C16:0e/18:1 PIe	1±0.11	1.10±0.22	1.18±0.12	1.07±0.12
C16:0/C18:1 PI	1±0.14	0.99±0.17	1.02±0.12	1.03±0.13
C16:0e/20:4 PIe	1±0.09	1.44±0.25	1.27±0.18	1.56±0.22
C18:0e/C18:1 PIe	1±0.22	0.95±0.44	0.70±0.24	0.60±0.12
C16:0/C20:4 PI	1±0.13	0.99±0.14	1.04±0.11	1.03±0.11
C18:0/C18:1 PI	1±0.13	1.04±0.17	1.01±0.11	1.05±0.13
C18:0e/C20:4 PIe	1±0.16	0.88±0.12	0.99±0.11	1.01±0.12
C18:0/C20:4 PI	1±0.15	0.99±0.14	1.09±0.12	1.07±0.12
C18:0/C18:2 PI	1±0.11	1.24±0.08	1.16±0.07	1.21±0.19
C16:0/C22:6 PI	1±0.07	0.48±0.03[a]	1.16±0.06	0.66±0.12[a]
C18:0/C22:6 PI	1±0.10	0.32±0.02[a]	1.16±0.07	0.44±0.12[a]
C16:0/C22:6 PC	1±0.05	0.45±0.01[a]	0.83±0.09	0.54±0.07[a]
C18:0/C20:5 PC	1±0.05	0.87±0.02[a]	0.92±0.04	0.92±0.07
C18:0/C22:6 PC	1±0.05	0.46±0.01[a]	0.87±0.09	0.57±0.07[a]
C18:0/C18:2 PC	1±0.04	1.20±0.05[a]	0.96±0.05	1.19±0.11
C16:0/C18:2 PC	1±0.06	1.66±0.03[a]	1.19±0.11	1.83±0.22[a]
C16:0/C20:5 PC	1±0.06	1.25±0.05[a]	1.18±0.07	1.32±0.14
C18:0e/C18:1 PCe	1±0.07	1.06±0.11	0.94±0.05	1.00±0.07
C16:0/C20:4 PC	1±0.02	1.34±0.04[a]	0.96±0.06	1.28±0.07[a]
C18:0/C18:1 PC	1±0.05	0.98±0.07	0.92±0.06	0.96±0.06
C18:0p/C20:4 PCp	1±0.04	1.00±0.06	0.90±0.07	1.06±0.04
C18:0e/C20:4 PCe	1±0.04	1.14±0.06	0.94±0.06	1.08±0.06
C16:0e/C18:1 PCe	1±0.06	1.22±0.15	0.97±0.10	1.12±0.08
C16:0/C18:1 PC	1±0.04	1.04±0.08	0.90±0.06	0.97±0.06
C16:0p/C20:4 PCp	1±0.05	0.85±0.05	0.85±0.06	0.90±0.06
C16:0e/C20:4 PCe	1±0.04	1.18±0.06[a]	0.95±0.06	1.21±0.05[a]
C18:0/C20:4 PC	1±0.04	1.26±0.07[a]	0.96±0.08	1.21±0.09
C16:0/C22:6 PG	1±0.06	1.61±0.10[a]	0.98±0.13	1.58±0.28
C18:0/C20:5 PG	1±0.04	1.42±0.10[a]	1.03±0.13	1.36±0.24
C18:0/C22:6 PG	1±0.07	1.45±0.09[a]	1.02±0.12	1.46±0.23
C16:0/C18:2 PG	1±0.06	0.74±0.05[a]	0.84±0.03[b]	0.79±0.08
C18:0/C18:2 PG	1±0.06	0.62±0.03[a]	0.85±0.05	0.70±0.07
C16:0/C20:5 PG	1±0.07	1.62±0.07[a]	1.05±0.12	1.63±0.27
C16:0/C20:4 PG	1±0.11	1.30±0.15	0.99±0.13	1.19±0.08

C18:0/C18:1 PG	1±0.08	0.48±0.06[a]	0.79±0.09	0.56±0.12
C18:0/C20:4 PG	1±0.17	1.26±0.07	0.89±0.11	1.27±0.07[a]
C16:0e/C20:4 PGe	1±0.16	0.95±0.18	0.88±0.21	0.70±0.11
C18:0e/C18:1 PGe	1±0.05	0.50±0.03[a]	0.81±0.10	0.57±0.08
C16:0/C18:1 PG	1±0.11	0.85±0.06	0.77±0.11	0.78±0.12
C16:0/C18:1 PS	1±0.09	1.05±0.07	0.98±0.06	1.10±0.07
C16:0/C18:2 PS	1±0.09	0.84±0.09	0.89±0.09	0.90±0.14
C18:0/C22:6 PS	1±0.06	0.78±0.04[a]	0.86±0.04	0.83±0.09
C18:0/C20:5 PS	1±0.06	0.93±0.05	0.96±0.05	1.01±0.10
C16:0/C22:6 PS	1±0.10	0.81±0.09	0.93±0.06	0.87±0.12
C18:0/C18:2 PS	1±0.06	0.98±0.05	0.92±0.04	1.01±0.13
C18:0e/C20:4 PSe	1±0.07	1.26±0.11	0.92±0.03	1.24±0.09[a]
C16:0/C20:4 PS	1±0.07	1.13±0.07	1.08±0.07	1.20±0.08
C18:0/C18:1 PS	1±0.06	1.06±0.08	0.90±0.07	1.06±0.04
C18:0e/C18:1 PSe	1±0.06	1.09±0.08	1.00±0.05	1.07±0.03
C16:0e/C20:4 PSe	1±0.14	1.62±0.39	1.35±0.18	1.57±0.31
C18:0/C20:4 PS	1±0.07	2.03±0.12[a]	1.01±0.09	1.84±0.21[a]
C16:0/C20:5 PS	1±0.08	1.16±0.08	1.22±0.12	1.27±0.13
C16:0e/C18:1 PSe	1±0.10	1.07±0.09	0.89±0.09	1.03±0.07
C16:0e/C18:1 PEe	1±0.07	1.21±0.07	0.90±0.07	1.17±0.05[a]
C16:0/C18:1 PE	1±0.02	1.24±0.07[a]	0.85±0.07	1.08±0.03[a]
C16:0p/C20:4 PEp	1±0.04	2.09±0.09[a]	1.06±0.18	1.77±0.18[a]
C16:0e/C20:4 PEe	1±0.02	1.37±0.10[a]	0.97±0.07	1.27±0.08[a]
C18:0e/C18:1 PEe	1±0.07	1.05±0.08	0.90±0.08	1.01±0.09
C16:0/C20:4 PE	1±0.05	1.66±0.09[a]	0.95±0.09	1.50±0.12[a]
C18:0/C18:1 PE	1±0.03	1.09±0.11	0.82±0.07	0.96±0.04
C18:0/C20:5 PE	1±0.04	1.02±0.05	0.92±0.05	1.03±0.10
C16:0/C22:6 PE	1±0.04	0.46±0.02[a]	0.84±0.09	0.56±0.08[a]
C18:0/C18:2 PE	1±0.04	0.98±0.05	0.89±0.06	0.94±0.07
C16:0/C20:5 PE	1±0.04	0.92±0.04	0.89±0.06	0.94±0.07
C16:0/C18:2 PE	1±0.06	1.34±0.05[a]	0.97±0.07	1.45±0.16[a]
C18:0/C22:6 PE	1±0.05	0.41±0.02[a]	0.81±0.10	0.49±0.06[a]
C18:0p/C20:4 PEp	1±0.04	1.49±0.07[a]	0.98±0.08	1.29±0.07[a]
C18:0e/C20:4 PEe	1±0.05	1.45±0.10[a]	0.93±0.10	1.22±0.07[a]

C18:0/C20:4 PE	1±0.01	2.04±0.09[a]	1.00±0.17	1.80±0.18[a]
C16:0e MAGe	1±0.10	0.98±0.09	0.95±0.10	0.93±0.07
16:0 MAG	1±0.15	1.12±0.16	1.13±0.07	1.31±0.13
C18:1e MAGe	1±0.09	0.92±0.11	0.95±0.18	0.99±0.06
C18:0e MAGe	1±0.18	0.79±0.23	0.70±0.27	1.06±0.22
C18:2 MAG	1±0.19	1.31±0.22	1.24±0.14	1.47±0.25
C18:1 MAG	1±0.16	0.92±0.16	0.96±0.10	1.01±0.17
C16:0e/C2:0 MAGe	1±0.21	0.87±0.11	1.42±0.22	1.16±0.11
C18:0 MAG	1±0.21	0.98±0.12	1.40±0.23	1.20±0.13
C20:4 MAG	1±0.17	0.89±0.14	0.94±0.10	1.13±0.11
C18:1e/C2:0 MAGe	1±0.11	0.49±0.06[a]	0.78±0.12	0.66±0.13
C18:0e/C2:0 MAGe	1±0.10	0.91±0.12	0.91±0.11	0.95±0.07
C22:6 MAG	1±0.15	0.40±0.07[a]	0.82±0.14	0.54±0.10
C16:0/C18:1 DAG	1±0.05	1.28±0.16	0.80±0.10	1.11±0.05[a]
C16:0/C20:4 DAG	1±0.10	0.93±0.07	0.74±0.08	0.98±0.09
C18:0/C18:1 DAG	1±0.18	0.97±0.15	0.77±0.13	0.94±0.14
C18:0/C20:4 DAG	1±0.07	1.15±0.15	0.92±0.12	1.08±0.10
C16:0/C18:2 DAG	1±0.09	0.47±0.11[a]	0.88±0.11	0.50±0.08[a]
C16:0/C20:5 DAG	1±0.07	1.09±0.08	0.90±0.12	1.17±0.11
C18:0/CC18:2 DAG	1±0.10	0.49±0.04[a]	1.00±0.14	0.67±0.13
C18:0/C22:6 DAG	1±0.10	0.55±0.01[a]	0.83±0.07	0.58±0.08[a]
C16:0/C22:6 DAG	1±0.05	0.30±0.02[a]	0.74±0.11	0.37±0.09[a]
C16:0/C20:5 DAG	1±0.09	1.12±0.08	0.91±0.11	1.17±0.11
C18:0/C18:2 DAG	1±0.08	0.50±0.04[a]	1.01±0.14	0.70±0.13
C16:0/C16:0/C16:0 TAG	1±0.02	2.04±0.36[a]	1.14±0.09	1.60±0.23
C16:0/C18:1/C16:0 TAG	1±0.05	1.71±0.15[a]	1.03±0.08	1.51±0.16[a]
C16:0/C20:4/C16:0 TAG	1±0.06	1.78±0.41	0.91±0.09	1.29±0.14[a]
C18:0/C18:1/C18:0 TAG	1±0.02	1.45±0.08[a]	1.09±0.05	1.41±0.11[a]
C18:0/C18:0/C18:0 TAG	1±0.04	1.38±0.10[a]	1.19±0.05[b]	1.38±0.10
C18:0/C20:4/C18:0 TAG	1±0.06	1.58±0.08[a]	1.14±0.10	1.54±0.13[a]
C16:0/C18:2/C16:0 TAG	1±0.04	2.02±0.28[a]	1.02±0.09	1.56±0.19[a]
C16:0/C20:5/C16:0 TAG	1±0.07	1.69±0.09[a]	1.11±0.06	1.59±0.19[a]
C16:0/C22:6/C16:0 TAG	1±0.07	1.66±0.10[a]	1.09±0.07	1.60±0.18[a]
C18:0/C18:2/C16:0 TAG	1±0.08	1.37±0.07[a]	0.95±0.04	1.25±0.10[a]

C18:0/C20:5/C16:0 TAG	1±0.15	1.52±0.09[a]	1.32±0.04	1.56±0.18
C18:0/C22:6/C16:0 TAG	1±0.07	1.31±0.05[a]	1.12±0.05	1.29±0.07
C16:0 acyl carnitine	1±0.12	1.15±0.15	0.96±0.15	1.43±0.27
C18:0 acyl carnitine	1±0.13	1.08±0.15	0.96±0.15	1.42±0.19
C18:2 acyl carnitine	1±0.08	1.25±0.12	1.49±0.40	2.20±0.66
C20:5 acyl carnitine	1±0.07	0.83±0.05	1.00±0.12	0.82±0.07
C22:6 acyl carnitine	1±0.08	1.35±0.19	1.35±0.6[b]	1.66±0.22
Lanosterol	1±0.08	1.03±0.09	1.05±0.11	1.11±0.15
C16:0 Ceramide	1±0.14	0.96±0.09	0.92±0.07	0.99±0.07
18:0/C16:0 ceramide-1-phosphate*	1±0.15	0.85±0.20	1.44±0.25	1.08±0.19
sphingosine	1±0.10	0.89±0.11	1.00±0.06	1.08±0.06
sphinganine	1±0.12	0.81±0.09	1.07±0.11	0.98±0.13
C16:0 SM	1±0.10	1.07±0.10	0.98±0.05	1.10±0.06
C18:1 SM	1±0.04	1.23±0.08[a]	0.89±0.05	1.21±0.09[a]
C18:0 SM	1±0.11	0.91±0.08	0.93±0.05	1.02±0.04
C20:4 SM	1±0.05	1.54±0.05[a]	1.08±0.10	1.65±0.15[a]
C16:0 NAE	1±0.14	1.13±0.13	1.06±0.11	1.41±0.18
C18:1 NAE	1±0.12	0.95±0.09	0.93±0.08	1.01±0.10
C18:0 NAE	1±0.16	1.08±0.13	1.01±0.13	1.46±0.22
Cholesterol/cholesteryl esters	1±0.11	0.97±0.13	0.97±0.11	1.04±0.09

References

1. Ellis J, *et al.* (2010) Adipose acyl-CoA synthetase-1 (ACSL1) directs fatty acids towards β-oxidation and is required for cold thermogenesis. *Cell Metabolism* 12(1):53-64.
2. Bonetto A, Andersson DC, & Waning DL (2015) Assessment of muscle mass and strength in mice. *Bonekey Rep* 4:732.
3. Fleming SM, Ekhator OR, & Ghisays V (2013) Assessment of sensorimotor function in mouse models of Parkinson's disease. *J Vis Exp* (76).
4. Castro B & Kuang S (2017) Evaluation of Muscle Performance in Mice by Treadmill Exhaustion Test and Whole-limb Grip Strength Assay. *Bio-protocol* 7(8):e2237.
5. Ellis JM, Wong GW, & Wolfgang MJ (2013) Acyl Coenzyme A Thioesterase 7 Regulates Neuronal Fatty Acid Metabolism To Prevent Neurotoxicity. *Molecular and Cellular Biology* 33(9):1869-1882.

6. Barrenha GD & Chester JA (2007) Genetic Correlation Between Innate Alcohol Preference and Fear-Potentiated Startle in Selected Mouse Lines. *Alcoholism: Clinical and Experimental Research* 31(7):1081-1088.
7. Dimauro I, Pearson T, Caporossi D, & Jackson MJ (2012) A simple protocol for the subcellular fractionation of skeletal muscle cells and tissue. *BMC Research Notes* 5(1):513.
8. Counihan JL, *et al.* (2017) Chemoproteomic Profiling of Acetanilide Herbicides Reveals Their Role in Inhibiting Fatty Acid Oxidation. *ACS Chem Biol* 12(3):635-642.
9. Louie SM, *et al.* (2016) GSTP1 Is a Driver of Triple-Negative Breast Cancer Cell Metabolism and Pathogenicity. *Cell Chem Biol* 23(5):567-578.
10. Benjamin DI, *et al.* (2013) Ether lipid generating enzyme AGPS alters the balance of structural and signaling lipids to fuel cancer pathogenicity. *Proc Natl Acad Sci U S A* 110(37):14912-14917.
11. Bligh EG & Dyer WJ (1959) A rapid method of total lipid extraction and purification. *Can. J. Biochem. Physiol.* 37:911-917.
12. Pereyra AS, *et al.* (2017) Loss of cardiac carnitine palmitoyltransferase 2 results in rapamycin-resistant, acetylation-independent hypertrophy. *The Journal of biological chemistry*.